Invited Paper

Spatially- and Angle-multiplexed Holographic Random Access Memory

Fai Mok
Northrop Corporation
Electronics Systems Division
2301 W. 120th St.
Hawthorne, CA90251

Demetri Psaltis, and Geoffrey Burr
California Institute of Technology
Pasadena, CA91125

ABSTRACT

A 3-D holographic optical memory is described that combines spatially and angularly multiplexed storage to yield a storage capacity of approximately 10^{12} bits in a crystal with volume less than 100 cm^3. A non-mechanical scanning mechanism, consisting of acoustooptic deflectors and a segmented mirror, retrieves any stored hologram in a time equal to the acoustic delay through the aperture of the acoustooptic deflector.

2.INTRODUCTION

The traditional advantages of 3-D holographic memories are high storage density and parallel access capability. These features were recognized in the early 60's [1, 2, 3,4] and serious efforts towards the practical implementation of such memories were undertaken. Unfortunately, these efforts did not produce commercially viable memories. In recent years there has been a resurgence of interest in 3-D optical storage due to a considerable improvement in the understanding and availability of storage media, a dramatic improvement in optoelectronic components in general, and most importantly, the emergence of applications, such as image processing, neural networks, and data bases where the capabilities of these memories can be effectively utilized. This recent activity has culminated in the storage of 5×10^3, 320×220-pixel holograms in a medium of volume roughly equal to $2cm^3$ [5]. If spatial light modulators with 1 million pixels are used, then the storage density achievable today is in excess of 10^9 bits per cm^3. This storage capability has to be compared with the density of other technologies, but most importantly the capabilities of random access semiconductor memories. Experimental RAM chips with 64 megabits have been demonstrated [6]. In other words, 16 such chips mounted on a board could replace a holographic memory with a volume equal to 1 cm^3. Therefore, it is imperative, if optical memories are to be competitive, that systems with much higher volume than 1 cm^3 are constructed with as high storage density as possible. Spatial multiplexing is the most straightforward way to increase the volume in which information is stored. Spatial multiplexing, in which angularly superimposed holograms are recorded at multiple spatial locations [3,7], automatically implies a scanning mechanism to address the different locations. We can use either mechanical or non-mechanical scanning. Non-mechanical spatial scanning is generally much faster, being able to access any one of the stored holograms in a time approximately equal to the access time of simple angle-multiplexed holographic memories. Several non-mechanical scanning mechanisms have been previously described [3,7].

0-8194-0946-4/93/$4.00

In this paper we describe a angle- and spatially-multiplexed memory with storage capacity approaching 10^{12} bits in a crystal with a volume of 64 cm^3, and random hologram-access time of $10 - 100$ μs. The key aspect of our memory is the non-mechanical scanning system we employ that makes use of acoustooptic deflectors in conjunction with a segmented mirror which allows us to perform both angular and spatial scanning.

3.ARCHITECTURE

The overall system is shown in Figure 1. We will describe this architecture with specific numbers for most of the relevant quantities. Obviously, the system can be redesigned with different numbers. The numbers we quote are based on what we believe is possible to fabricate with currently available technology. The storage medium is a photorefractive crystal such as $LiNbO_3$ (item 1 in Figure 1). Holograms are stored in multiple locations on the crystal. The locations are arranged in a regular 16 by 16 grid. Each location stores up to 4,000 holograms.

The vertical AOD in the reference arm of the system (item 4 in Figure 1) steers the reference beam to the location on the crystal where a hologram is to be written. This AOD deflects the collimated light vertically to one of the elements in the array of 256 mirror strips that are stacked vertically. This segmented mirror is marked as item 6 in Figure 1. Each of the mirror strips has a unique orientation. The orientation of each mirror strip is designed to redirect the incident light (both horizontally and vertically) to one of the 16×16 locations on the $LiNbO_3$ crystal. In this way, the deflection angle of the vertical AOD specifies which mirror strip is illuminated which in turn selects the location of the reference beam on the crystal. Figure 2a shows how the combination of the vertical AOD (item 4 in Figure 1) and the segmented mirror directs the reference beam to different locations on the storage medium. Figure 2b shows the horizontal AOD (item 5 in Figure 1) and one of the strips of the segmented mirror, demonstrating how the angle of the reference beam is scanned in the horizontal direction.

The horizontal AOD (item 5) is used to deflect the beam horizontally. The horizontally deflected light remains on the same mirror strip as long as the vertical deflection remains the same. Notice that since the segmented mirror is in the Fourier plane of the crystal, this means that the position of the reference beam on the crystal also remains unchanged. The deflection by the horizontal AOD changes the angle of incidence of the reference beam on the crystal which provides the multiple angles needed for the angular multiplexing of the superimposed holograms. In this way, the vertical AOD (via the segmented mirror) selects the location of the reference beam on the crystal, whereas the horizontal AOD selects the angle of incidence of the reference beam.

The mirror stack will be fabricated by employing the technique used for making blazed gratings. This technique involves using a diamond tip to cut grooves on suitable substrates (see Figure 3). The angles of the grooves are accurately controlled by the tilt of the diamond tip with respect to the substrates. The width of each groove is controlled by the number of cuts in the same groove.

The number of mirror-strips is equal to the number of distinct locations within the storage medium. There are, therefore, 16×16 mirror strips within the mirror stack. The mirror stack is composed of 16 sub-stacks. Each sub-stack consists of 16 mirror strips (Figure 4a). The change in angle from one strip to the next is 0.5°. The 16 sub-stacks are identical except that ramps are cut out of the substrates of the sub-stacks (Figure 4b). The difference in ramp angles between neighboring sub-stacks is also 0.5°. Note that the direction of angular change of the substrate ramps is orthogonal to that of the mirror strips so that a two-dimensional spatial scanning is possible. These requirements can be met by blazed grating manufacturing technology.

Figure 5 shows the spatial multiplexing of the data (object) beam in one dimension. (Spatial multiplexing in the other dimension is identical.) In order to store the holograms in the crystal, each page is first displayed at the input SLM. The size of the pages is limited by the space-bandwidth-product (SBP) of the SLM. The SLM is illuminated by a plane wave whose angle of incidence is determined by the signal applied to the AOD. The light at the SLM and the crystal planes are a Fourier transform pair. Therefore, we can shift the location where the light is focused on the crystal by changing the angle of SLM illumination. In other words, the AODs control which location on the crystal is being written. During recording, the electrooptic phase modulators (item 7 and 8 in Figure 1) will compensate the frequency shifts introduced by the AODs.

The set-up in Figure 5a requires that the AOD has a SBP of M×N, where M is the number of locations and N is the SBP of the SLM in one dimension. In the case that M=16 and N=1,000, the SBP requirement on the AOD would be 16,000, which is clearly outside the reach of current technology. The SBP requirement on the AOD can be alleviated by using two 16×16-element lenslet arrays as shown in Figure 5b. In such case, the SBP required of the AOD is reduced to MNf_2/f_1.

Each stored page is associated with a unique reference beam characterized by its angle of incidence and its location. Any one of the stored pages can be accessed by simply illuminating the storage medium with the appropriate reference beam. This reference beam is generated by the same system used during the recording phase. The Fourier transform of the page associated with this reference beam will be reconstructed. An output detector array (Item 9 in Figure 1), which is at the Fourier plane of the storage medium, will register the image of the reconstructed page of information. A pulsed laser is used as the readout light source. Since sufficient photons are delivered in a compressed time slot, the access time is minimized. Firing of the laser is synchronized with the launching of the acoustic waves within the AOD. The laser is charged to full firing potential while data is read from the detector array.

The sufficient condition for data pixels to be resolvable at the detector plane is that the Fourier transform lenses (Item 10 and 11) in Figure 1 have SBPs in excess of MN or 16,000. Laser scanning lenses satisfying this specification will be used in our setup.

4.FOURIER TRANSFORM HOLOGRAMS

Most of the energy of the Fourier spectra of most positive definite images are distributed in the d.c. and the low frequency components (see Figure 6 for example). Therefore, when Fourier transform holograms are recorded, one of the following three situations will occur.

1. The reference beam intensity is low compared to the intensity of the low frequency components. The modulation depth (m) of the gratings corresponding to the low frequency components is small. Since grating amplitude is approximately proportional to m for small m, the low frequency components gratings are weak comparing to those of the high frequency components. As a consequence, the reconstruction of the hologram will show emphasis in the high frequency components.

2. The reference beam intensity is approximately equal to the intensity of the low frequency components. The modulation depth (m) is higher for low frequency components resulting in a reconstruction which emphasizes the low frequency components.

3. The reference beam intensity is much higher than the intensity of all frequency components. In this case, the reconstruction will be linear, but the overall diffraction efficiency will be low.

An example of a non-linear reconstruction is shown in Figure 7.

The energy distribution of the Fourier spectrum can be made more uniform by using a diffuser (Figure 8). If the diffuser only encodes phase information, there should be no excessive information loss at the output plane. To demonstrate the benefit of using a diffuser, 1,000 images of random-bit patterns were recorded and reconstructed. An example of the result is shown in Figure 9. It is evident from Figure 9 that the holographic storage was linear. Also notice that the white pixels are grainy which is believed to be caused by the non-ideal ground glass diffuser. The usage of a custom diffuser should eliminate most this diffuser noise. Even when present, this diffuser noise should not lower the signal to noise ratio of the output significantly since the output is obtained by integrating all the energy within a detector pixel.

5.HOLOGRAPHIC CROSS-TALK MEASUREMENTS

A potential source of error is holographic cross-talk, a result of the fact that the holograms share a common volume. In this section, however, we will show that this error source will not be dominant if proper precautionary steps are taken.

Cross-talk between holograms sharing a common volume was measured in the recording and reconstruction of 500 and 1,000 holograms. In these experiments, computer-generated, random-bit patterns were recorded as volume holograms within a single crystal of lithium niobate.

Reconstructed holograms were imaged onto a CCD camera. To increase the dynamic range of output detection, each reconstructed pattern *bit* was imaged onto approximately 6×6 CCD pixels. (The dynamic range of each CCD pixel is 8 bits or 256. By using 36 CCD pixels to detect a single reconstructed pattern pixel, the effective dynamic range for output detection was increased by 36-fold.) Imaging a pattern bit on *exactly* 36 CCD pixels was not attempted. As a result, a transition effect was observed on the boundary pixels of the 36 CCD pixels (Figure 10). To avoid this transition effect, only data from the central 4×4 CCD pixels, the inner square of the 6×6 pixels, were recorded. Data from the 20 boundary pixels were discarded.

A randomly selected unit of 4×4 CCD pixels was designated to be the output of the experiments. Randomly chosen holograms were reconstructed. Each time a hologram was reconstructed, 16 data points from the designated 16 CCD pixels were taken. These 16 data points were then summed to produce a single output data point to represent the output level of the corredponding pattern bit of the reconstructed hologram. Seventy such output data points from 70 reconstructed holograms were obtained. All pattern bits of logic level 1 produced output data points with large magnitudes and all pattern bits of logic level 0 produced output data points of small magnitudes. In other words, no errors were detected. These data points were averaged to produce the following results.

$$[\text{logic } 1]_{avg} = 2940,$$

and

$$[\text{logic } 0]_{avg} = 0.56,$$

where $[\text{logic } 1]_{avg}$ is the average signal level and $[\text{logic } 0]_{avg}$ is the average cross-talk level. The average signal-to-cross-talk ratio was, therefore,

$$\frac{[\text{logic } 1]_{avg}}{[\text{logic } 0]_{avg}} = 5250.$$

The standard deviation, σ, of the cross-talk was 1.8. Assuming an error function distribution for the cross-talk, the projected bit-error rate was

$$Erf\left(\frac{\theta - 0.56}{1.8}\right) = \int_{\theta}^{\infty} G(0.56, \sigma),$$

where θ is the threshold level, 0.56 is the average cross-talk level, and $G(.,.)$ is the gaussian function. 10^{-12} is the industrial standard for bit-error rate. (The raw data bit error-rate of optical disks is actually only 10^{-6}; 10^{-12} is achieved using error correction codes.) To achieve this bit error-rate, we need a threshold value of

$$\theta = 13.2$$

which is only 1/223 of the average signal level. This huge difference between the required threshold and the average singal level means that the contribution to bit-error rate due to holographic cross-talk is insignificant.

Another potential source of error is the fluctuation of diffraction efficiencies among the holograms. For example, diffracted light intensity from some logic 1 pattern bits may be lower than the threshold level and may, therefore, be incorrectly classified as logic 0. Such an error will be extremely rare since the diffracted light intensity has to drop from an average value of 2,940 to 13.2 for this to happen. Using the same threshold level of 13.2, the bit-error rate attributed to diffraction efficiency fluctuation is calculated to be

$$Erf\left(\frac{13.2 - 2,940}{248}\right) < 10^{-28},$$

which far exceeds the industrial standard of 10^{-12}. Also, note that diffraction efficiency fluctuation can be eliminated by using automatic gain control at the output.

The above results were obtained from the 500-hologram experiment. Results from the 1,000-hologram experiment suggested an even lower bit error-rate. The majority of the cross-talk from the 500-hologram experiment was found to have been caused by inexact Bragg-matching during reconstruction of the holograms. (The translation stage used for steering the reference beam to reconstruct holograms has a 5% repeatability error.) Special care was, therefore, taken to manually Bragg-match the reconstructions of the holograms in the 1,000-hologram experiment. The average noise level was measured to be 0, with a standard deviation of also 0. This result, of course, does not suggest that cross-talk did not exist. It does, however, indicate that our experimental set-up was not sensitive enough to measure the cross-talk.

6.ACKNOWLEDGEMENTS

This work is funded by Rome Lab/IRAP under contract F30602-92-C-0073.

7.REFERENCES

1. P.J. Van Heerden, *Appl. Optics*, **2**, 393 (1963).

2. J.J. Amodei and D.L. Staebler, *Appl. Phys. Lett.*, **20**(2), 79 (1972).

3. J. P. Huignard, F. Micheron, and E. Spitz, "Optical Systems and Photosensitive Materials for Information Storage", in *Optical Properties of Solids*, B.O. Seraphin, editor, Chapter 16, pages 847-925, North Holland, Amsterdam, 1976.

4. R.A. Bartonlini, A. Bloom, and J.S. Escher, *Appl. Phys. Lett.*, **28**, 506 (1976).

5. Fai H. Mok and Harold M. Stoll, "Holographic Inner-product Processor for Pattern Recognition", *Proc. SPIE*, **1701**, 312 (1992).

6. Y. Nakagome, et al., *IEEE J. Solid State Circuits*, **26**(4), 465 (1991).

7. F.M. Smits and L.E. Gallaher, *Bell System Technical Journal*, volume XLVI, 1267(1967).

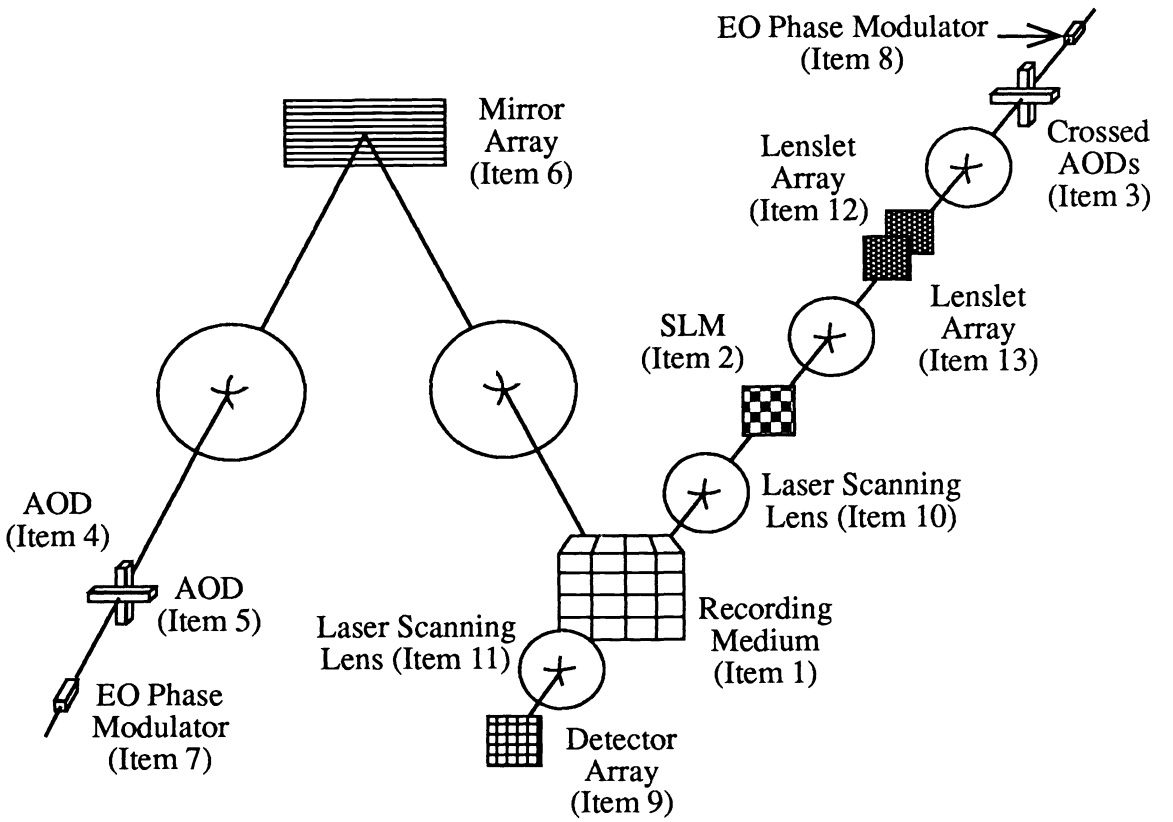

Figure 1. Schematic diagram of spatially- and angle-multiplexed holographic random access memory.

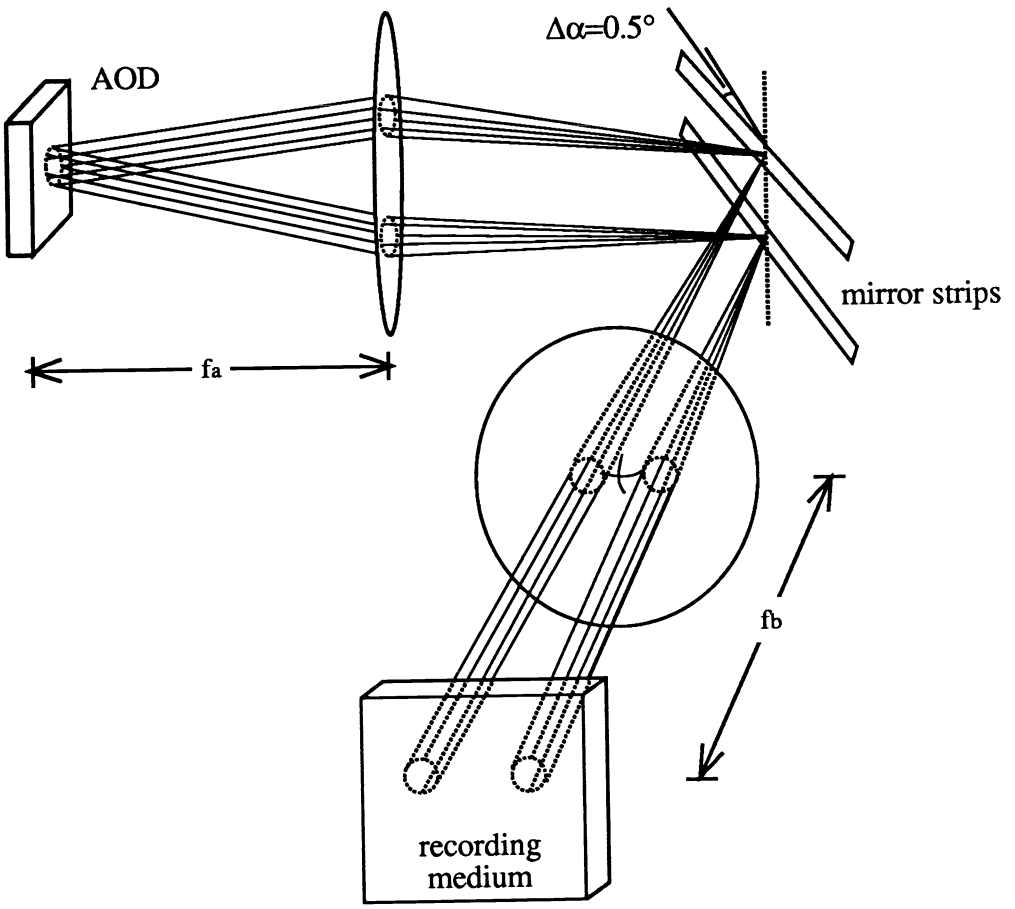

Figure 2a. A two-element mirror stack, opterating in conjuction with a vertically-oriented AOD and wo lenses, redirects light to two distinct locations within the storage medium.

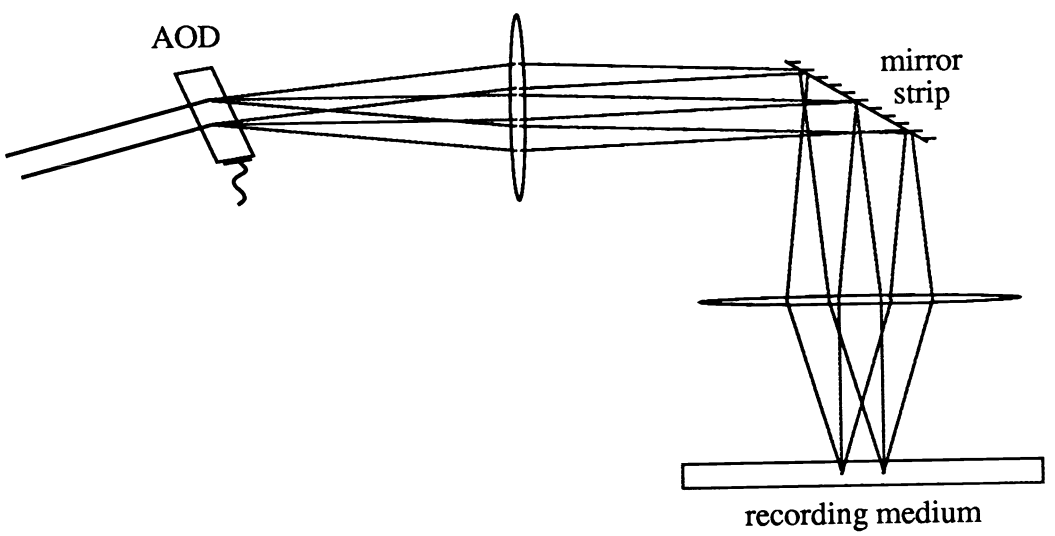

Figure 2b. Schematic diagram showing three collimated beams with different angles of incidence on the storage medium. Note that all three beams stay within a common location.

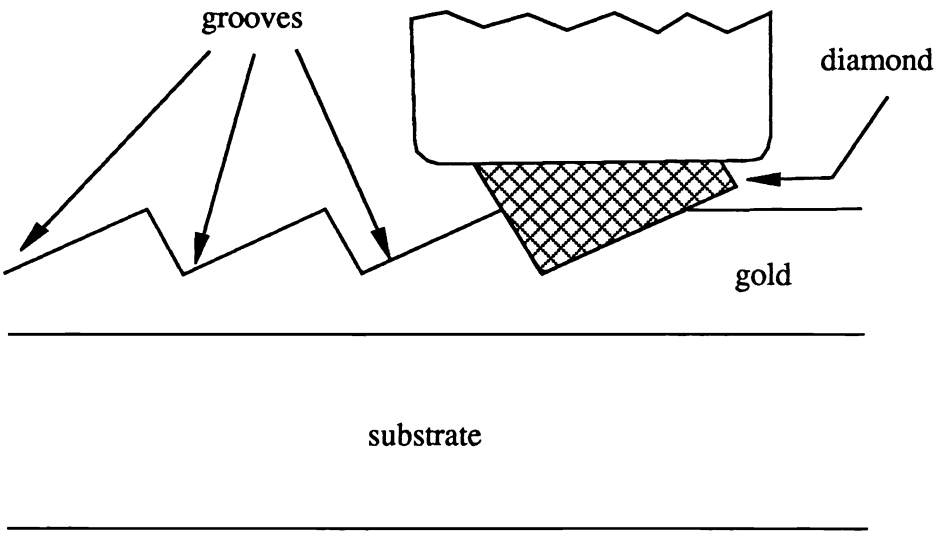

Figure 3. A simplified diagram showing the fabrication of a blazed grating.

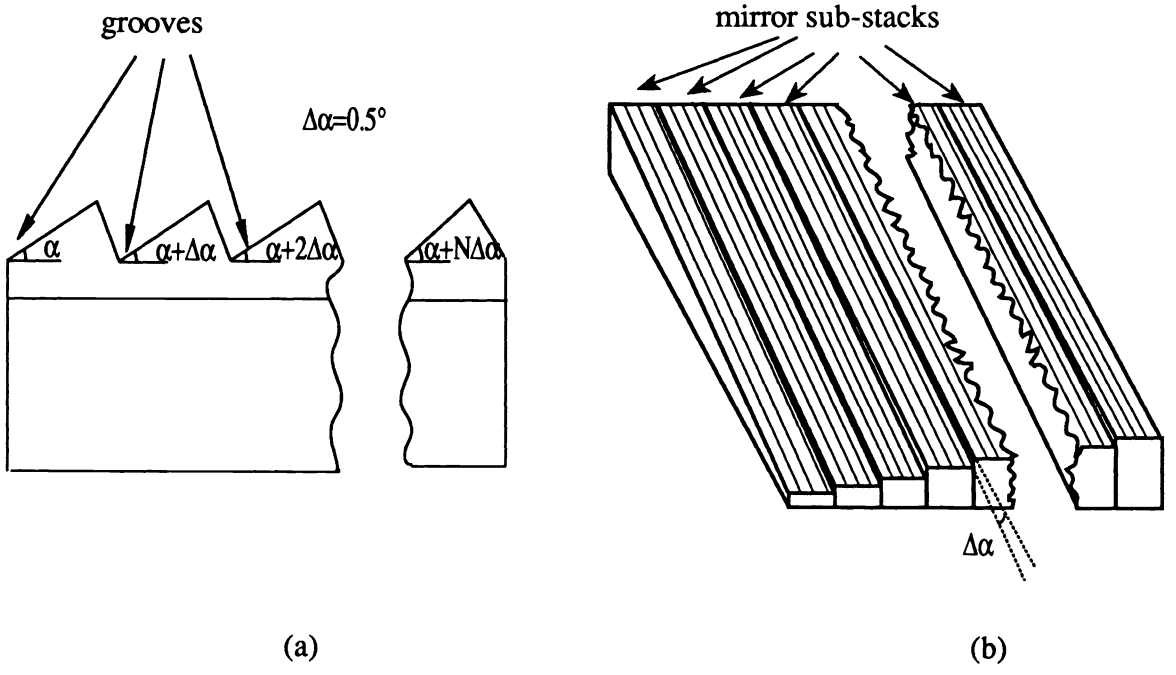

Figure 4. (a) Cross-sectioned profile of a mirror sub-stack. Each sub-stack has N mirror strips. (b) A mirror stack is made from N identical sub-stacks. Ramps of different angles are cut from the substrates of the sub-stacks. Therefore, each of the N×N mirror strips has a unique orientation.

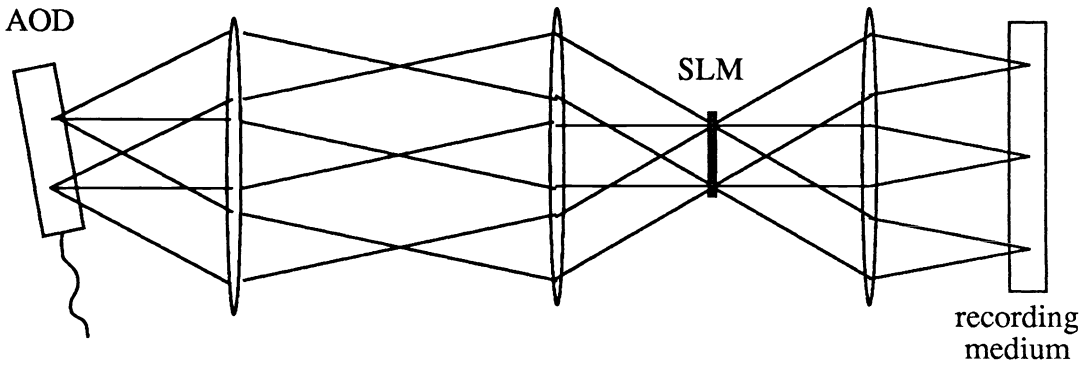

(a)

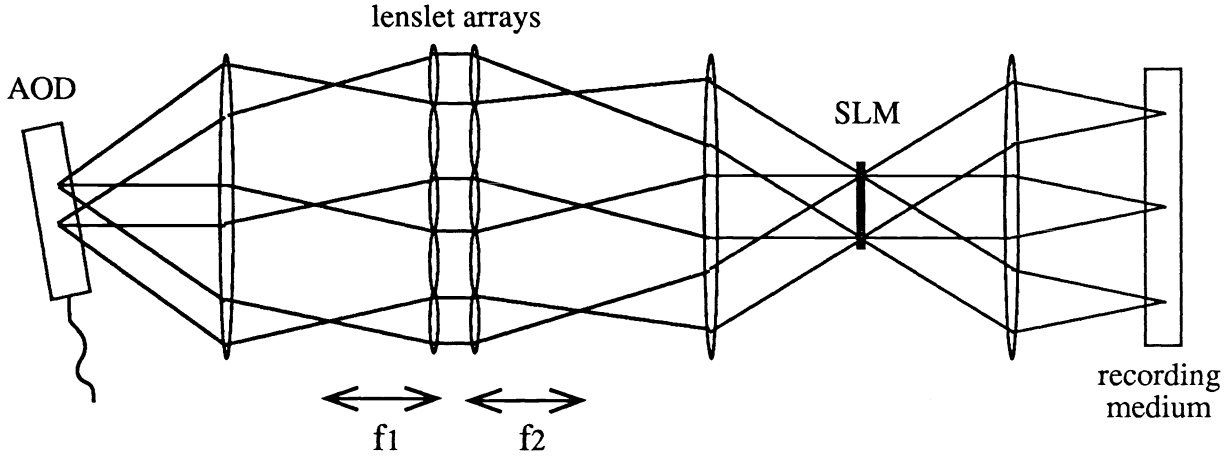

(b)

Figure 5. Fourier transforms of SLM images are spatially multiplexed onto different locations within the recording medium by changing the angle of incidence of the collimated beam illuminating the SLM. (a) The SBP requirement on the AOD is MN. (b) The SBP requirement on the AOD is MNf_2/f_1.

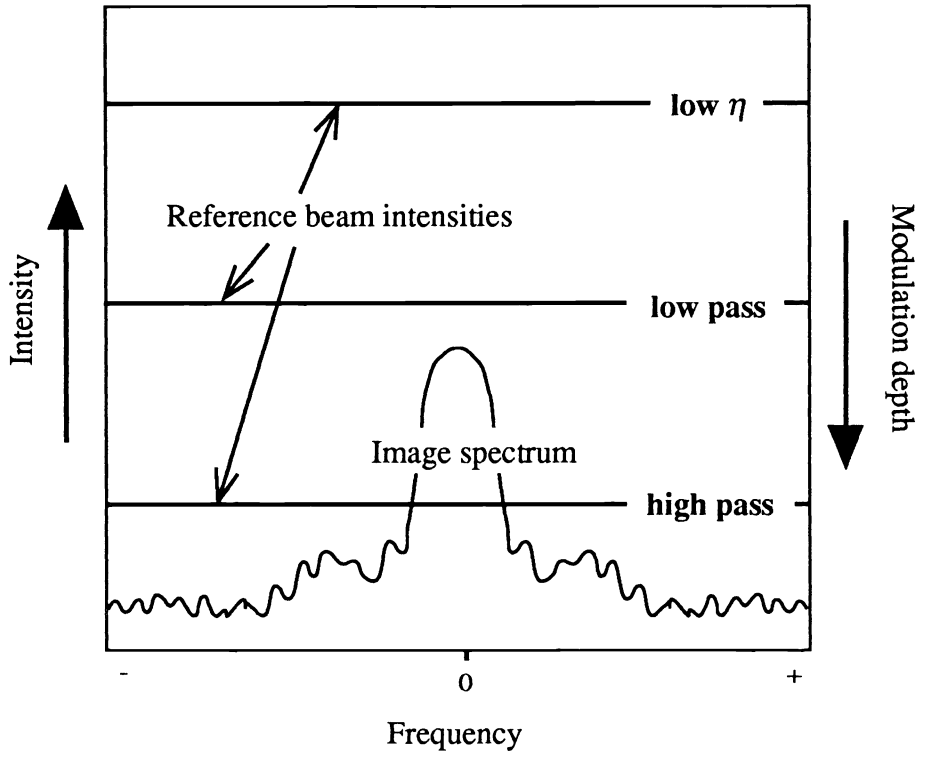

Figure 6. Non-linear effects in reconstruction of Fourier transform holograms due to high-energy low frequency components.

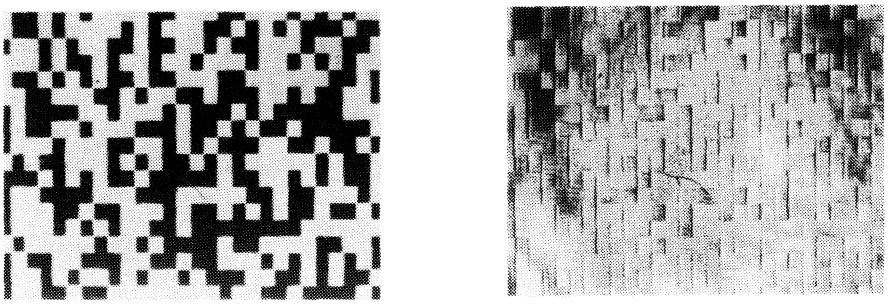

Original Reconstruction

Figure 7. An example demonstrating the non-linear reconstruction of a Fourier transform hologram.

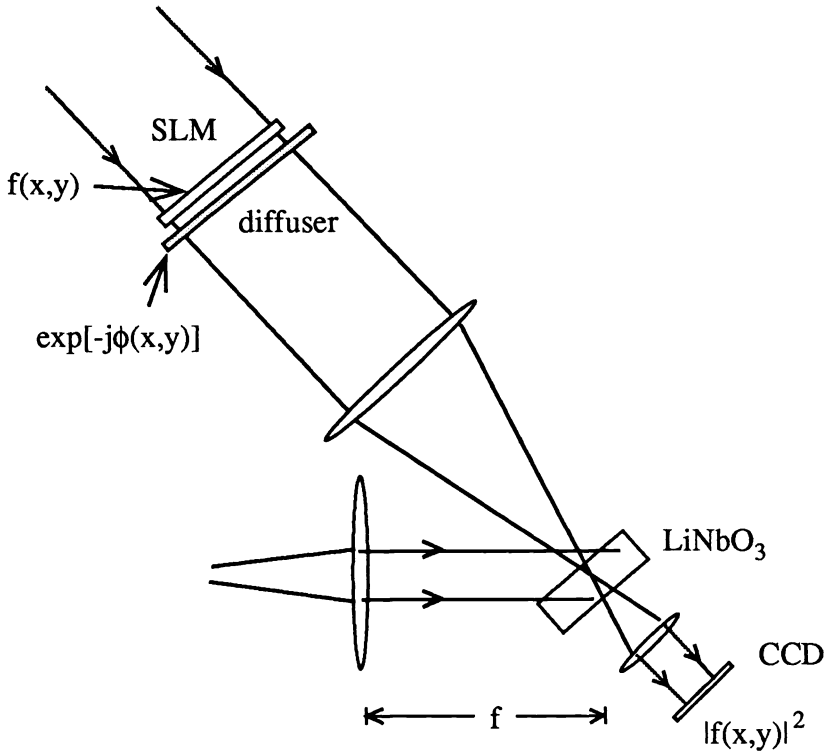

Figure 8. Schematic diagram dipicting the usage of a diffuser in a Fourier holographic set-up.

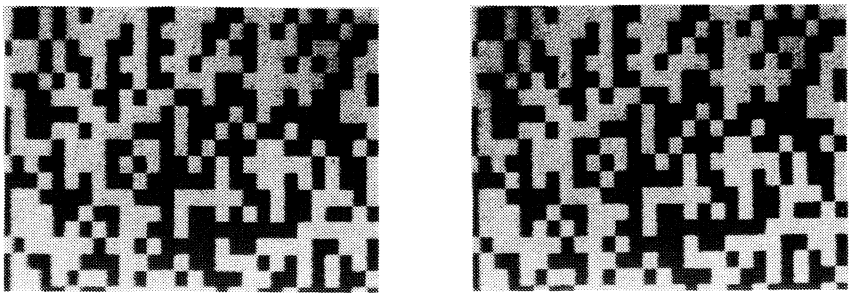

Original Reconstruction

Figure 9. A sample reconstruction from a sequence of 1,000 Fourier holograms recorded using the set-up in Figure 8.

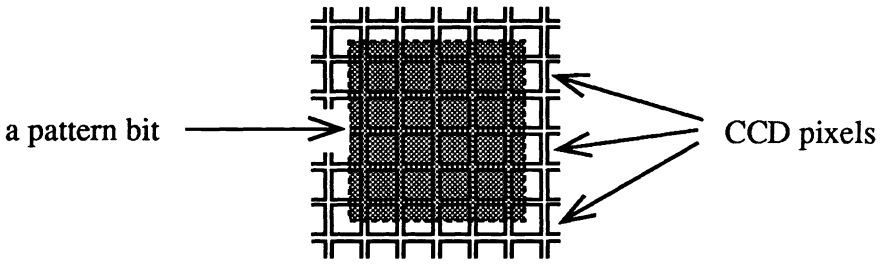

Figure 10. The shaded region represents the image of a SLM pattern bit on the CCD. Notice that each pattern bit covers more than 4×4 CCD pixels.